CHAPTER SIX

ELECTRICAL PROPERTIES OF ZnS_xSe_{1-x} THIN FILMS

6.1 Introduction

The electrical properties of ZnS, ZnSe and Zns_xSe_{1-x} materials have been intensively studied [12, 13, 30-35, 42, 46, 48, 52, 126]. These properties were found to be strongly dependent on the method and conditions of preparation. For instance, the dark conductivity at room temperature for $ZnS_{0.25}Se_{0.75}$ crystals, prepared by vapour transport growth, was found [46] to vary from 10^{-14} to 10^{-12} $(\Omega cm)^{-1}$. This variation of conductivity was attributed to the increase of native defects such as zinc vacancy. However, high conductive zinc sulphoselenide films have been obtained [48] by using hydrogen vapour transport deposition. The conductivity of these films has been reported to be in the range of $1\text{-}10^{-3}$ $(\Omega cm)^{-1}$ depending upon zinc partial pressure of the growth ambient and sulphur concentration in the film. The electronic properties of the self-activated (SA) center in ZnS_xSe_{1-x} alloys, prepared by iodine vapour transport technique, were studied [52] using junction space-charge techniques. The temperature dependence of the carrier concentration and Hall mobility has been studied for ZnSe [31, 34, 35] and the conductivity of the as-grown films grown expitaxially on p-type GaAs substrates, was found [35] to be in the range of $10\text{-}10^{-5}$ $(\Omega cm)^{-1}$. The temperature dependence of the intrinsic conductivity was studied [12] for hexagonal ZnS single crystals and activation energy of 3.77 eV was obtained. The electronic properties of low resistive n-type ZnS crystals were studied [13] and the room-temperature conductivity in the range of 1-0.1 $(\Omega cm)^{-1}$ was obtained.

In this chapter the electrical properties of ZnS_xSe_{1-x} thin films grown by electron beam evaporation onto glass substrates at 60^0 C will be presented. In this study, the current voltage (I-V) characteristics were investigated at temperature range of 30 - 475 K. The temperature dependence of the dc-conductivity was investigated by measuring the current passing through the sample as a function of ambient temperature at fixed applied voltage (V=10 V). The model proposed by Mott and Davis [72] was employed to explain the variation of conductivity with temperature and to estimate the activation energies. The effect of film structure, such as sulphur concentration, film thickness and grain size, on the activation energy and the conductivity of ZnS_xSe_{1-x} samples was investigated.

6.2 Current-Voltage (I-V) characteristics

Figures 6.1 (a-d) and 6.2 (a-d) show typical current-voltage (I-V) characteristics for ZnS_xSe_{1-x} thin films studied in this work at different ambient temperatures in the ranges of 30 - 250 K and 300 - 475 K, respectively. Similar (I-V) characteristics were obtained for the other ZnS_xSe_{1-x} samples investigated in this work where a linear relation between the current and the applied voltage is observed. At high temperature ($T \geq 400$ K), however, this relation deviates from the linearity for some samples (see Figures 6.2 (b) and (d)). The linear behaviour of the current, as a function of the applied voltage, indicates that the number of the thermally generated free carriers exceeds the density of the injected charge carriers from the electrode [127]. It also confirms that good ohmic contact between the electrodes and the film was obtained [128]. Space charge limited current (SCLC) conduction mechanism, where the current is proportional to V^2 [127], was not observed in the range of voltage and temperature used in this work. The non-linear behaviour that is observed for some samples at high temperatures can be attributed to the Poole-Frenkel

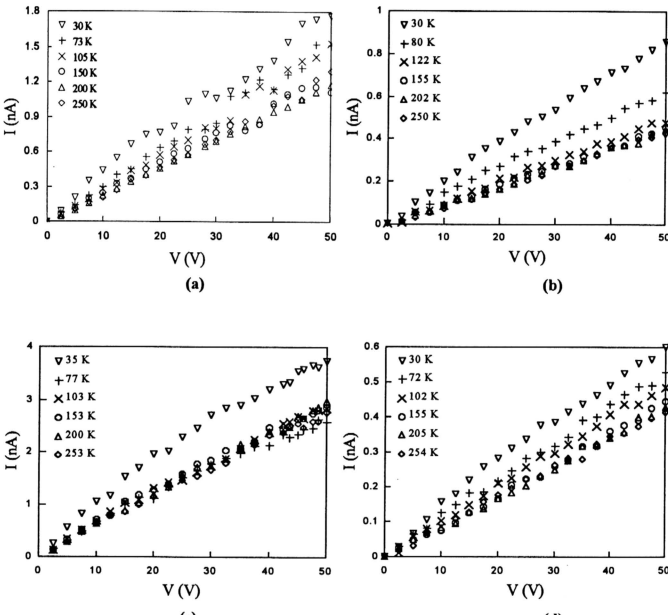

Figure 6.1: I-V characteristics at different temperatures for ZnS_xSe_{1-x} thin films, prepared by electron beam evaporation onto glass substrates at 60 ° C, with x values: 0.80 **(a)**, 0.90 **(b)**, 0.96 **(c)** and 1.0 **(d)**.

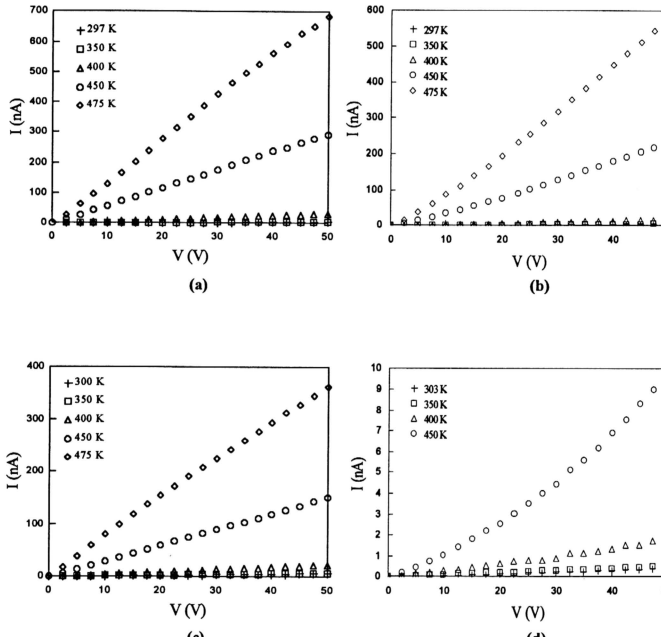

Figure 6.2: I-V characteristics at different temperatures for ZnS_xSe_{1-x} thin films, prepared by electron beam evaporation onto glass substrates at 60 ° C, with x values: 0.12 **(a)**, 0.41 **(b)**, 0.82 **(c)** and 1.0 **(d)**.

effect or the Schottky effect, where the current in the film increases more rapidly than the applied field [72]. Schottky effect is the attenuation of a metal-insulator potential barrier arising from electrode image-force interaction with the applied electric field while in the Poole Frenkel effect the applied field lowers the ionization potential energy of the trap [72, 129]. Both of these effects give the conductivity σ field dependence as [71, 129]

$$\sigma = G_0 \exp\left[\frac{-e\phi_B + \beta' F^{1/2}}{K_\beta T}\right] \quad \text{.....(6.1)}$$

where G_0 is a constant with the dimension of conductivity, e is the electronic charge, ϕ_B is the barrier height for emission from the metal electrode in the Schottky effect or from trap in the Poole-Frenkel effect, β' is a constant, F is the applied electric field strength, K_β is Boltzmann's constant and T is the absolute temperature. For the Pool-Frenkel effect $\beta' = \beta_{PF} = (e^3 / \pi\varepsilon_0\varepsilon')^{1/2}$, where ε' is the high frequency dielectric constant of the sample and ε_0 is the permittivity of free space. The factor β' is given for the case that only donors are present. If acceptors were also present, β' would be larger by a factor of 2 [130]. For the Schottky effect $\beta' = \beta_s = \beta_{PF} / 2$.

To examine the validity of equation (6.1), for the samples in which the (I-V) characteristics deviate from the linearity, the dc-conductivity σ has been calculated from (I - V) characteristics according to the relation

$$\sigma = \frac{L}{Wt}\frac{I}{V} \quad \text{.....(6.2)}$$

where L is the separation between the planar electrodes, W is the width of the electrode, t is the geometrical thickness of the sample, I is the current that passes through the sample and V is the applied voltage. Figures 6.3 (a-d) and 6.4 (a-d) show the plots of ln (σ) versus $F^{1/2}$ according to equation 6.1 for ZnS_xSe_{1-x} thin films in the temperature range of 30 - 250 K and 300 - 475 K, respectively. It is seen from Figure 6.3 (a-d) that σ is independent of the electric field in the temperature range of 30 - 250 K. The fluctuations in σ values, which can be seen in Figure 6.3, might be due to the uncertainty in the current measured at low temperatures. In Figures 6.4 (a-d), the electric field independence of the conductivity is clearly observed at $T \geq 300$ K. This independence of σ confirms again the ohmic behaviour of the conduction except for the samples with $x = 0.41$ and 1.0 at high temperatures (see Figures 6.4 (b) and (d)) where σ shows electric field dependence. By fitting the data in Figures 6.4 (b) and (d) at high temperatures ($T \geq 400$ K) to equation (6.1), the value of the constant β' ($=K_\beta T$ × slope) was determined. These experimentally determined values of β' were compared with the theoretical values of β_{PF} and β_s for the Poole-Frenkel and Schottky effects, respectively, to estimate the high-frequency dielectric constant ε' of the materials.

The resulting values of ε' for $ZnS_{0.41}Se_{0.59}$ and ZnS are shown in Table 6.1. The values of the dielectric constant ($\varepsilon' = \varepsilon'_{PF}$) as determined according to the Poole-Frenkel effect with the assumption that both donors and acceptors are present in the samples are more acceptable than either the values determined according to the presence of the donors only ($\varepsilon' = \varepsilon''_{PF}$) or according to the Schottky effect ($\varepsilon' = \varepsilon'_s$) (see Table 6.1). The large values of ε'_{PF} at 400 K indicates that the value of β', which has been determined from the slopes in Figures 6.4 (b) and (d), is quite small and hence

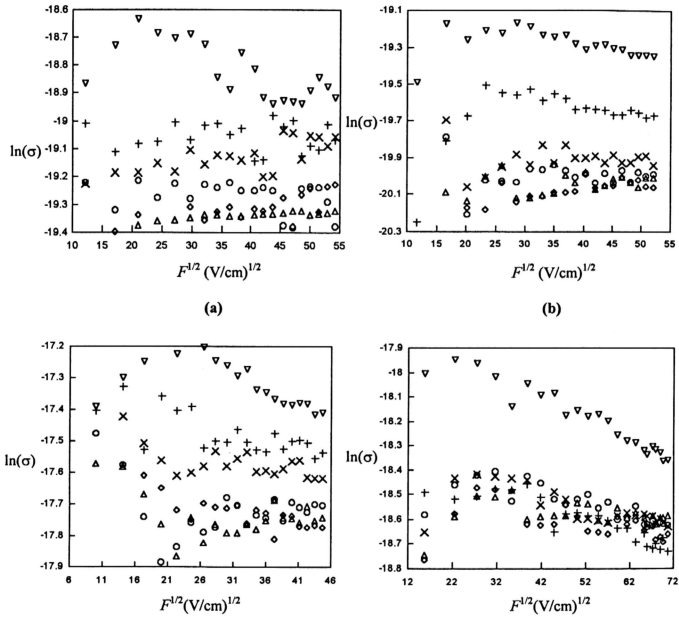

Figure 6.3: ln (σ) in $(\Omega.cm)^{-1}$ versus $F^{1/2}$ in $(V/cm)^{1/2}$ for ZnS_xSe_{1-x} films, (with x values: 0.80 **(a)**, 0.90 **(b)**, 0.96 **(c)** and 1.0 **(d)**), at temperatures 30 ▽, 75 +, 103 ×,153 ○ , 200 △ and 250 K ◇.

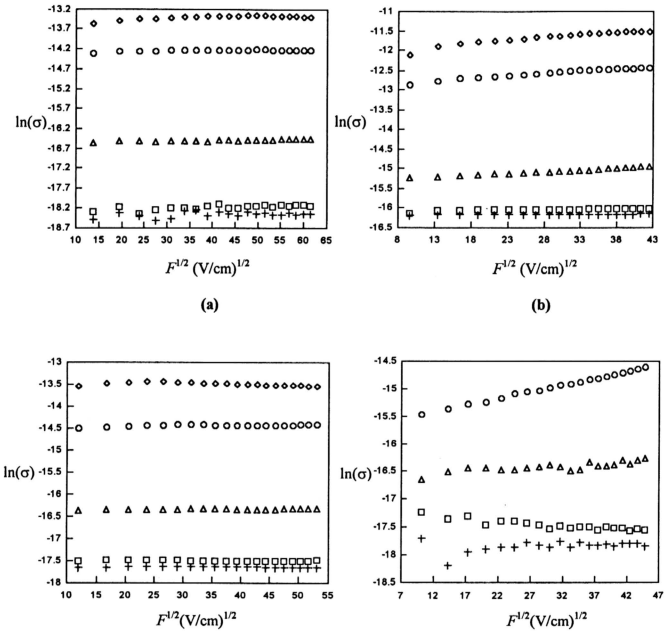

Figure6.4: ln (σ) in $(\Omega.cm)^{-1}$ versus $F^{1/2}$ in $(V/cm)^{1/2}$ for ZnS_xSe_{1-x} films, (with x values: 0.12 **(a)**, 0.41 **(b)**, 0.82 **(c)** and 1.0 **(d)**), at temperatures 300 +, 350 □ , 400 △, 450 ○ and 475 K ◇.

the variation of σ with F is too small to be considered as a Poole-Frenkel effect. The values of ε'_{PF} at 450 and 475 K however are somewhat lower than the expected values (ε'=5.13 for ZnS [64] and 9.1 for ZnSe [36] as determined at room temperature). The adoption of the Poole-Frenkel effect means that the conduction mechanism is bulk-limited rather than electrode-limited [129]. However, values of ε' as determined from the Poole-Frenkel effect have been reported to be lower than the optically determined ones for other materials [129, 131]. The low values of ε'_{PF} can be explained by the field being uniform across the sample as carriers are trapped. This effect is most pronounced at the lowest fields where detrapping is least likely, and therefore the slope of the Poole-Frenkel plot increases [131]. In order to determine the trap depth ϕ_B [131], ln σ (as determined from equation 6.2) was plotted against (1000/T) as shown in Figure 6.5 for $ZnS_{0.41}Se_{0.49}$ and ZnS samples at electric fields of 360 and 400 V/cm, respectively. It can be seen from Figure 6.5 that equation 6.1 is not valid for approximately $T < 400$ K. The data for $T \geq 400$ K were fitted to the Poole-Frenkel equation (equation 6.1) where ϕ_B was estimated from the slope of the line in Figure 6.5 such as

$$e\phi_B = 1000 \times K_B \times slope - \beta' F^{1/2} \quad \text{.....(6.3)}$$

A small error might be introduced by following this procedure to determine ϕ_B because β' in equation 6.3 has a slight temperature dependence due to a temperature dependence in ε'_{PF} (see Table 6.1). Since the electric fields in Figure 6.5 are very small, the contribution of the electric field in equation 6.3 ($\beta' F^{1/2} < 0.018$ eV) is negligible, and hence the temperature dependence of β' will produce a negligible error in the value of ϕ_B in equation (6.3). The values of ϕ_B were estimated according to

Table 6.1: The experimentally determined values of β for $ZnS_{0.41}Se_{0.59}$ and ZnS samples at high temperatures and the corresponding high-frequency dielectric constants ε'_{PF}, ε''_{PF} and ε'_s, according to the Pooe-Frenkel and Schottky effects, respectively.

	$x = 0.41$				$x = 1.0$			
T(K)	$\beta \times 10^4$ eV(cm/V)$^{1/2}$	ε'_{PF}	ε''_{PF}	ε'_s	$\beta \times 10^4$ eV(cm/V)$^{1/2}$	ε'_{PF}	ε''_{PF}	ε'_s
400	3.032	25.1	6.3	1.567	2.314	43.1	10.8	2.692
450	5.152	8.7	2.2	0.543	9.412	2.6	0.7	0.163
475	5.562	7.5	1.9	0.466	----------	------	------	-------

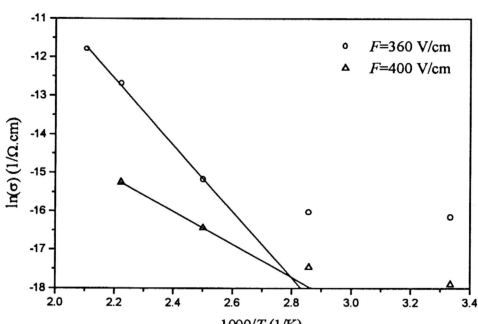

Figure 6.5: ln(σ) versus (1000/T) for $ZnS_{0.41}Se_{0.49}$ o and ZnS Δ films (see the enclosed values of the applied electric field F) prepared by electron beam evaporation onto glass substrates at 60 ^{0} C.

equation (6.3), as 0.75 eV and 0.37 eV for $ZnS_{0.41}Se_{0.49}$ and ZnS, respectively. The value of ϕ_B (0.37 eV) for ZnS is in a good agreement with the value 0.35 eV reported in reference [52].

6.3 Temperature dependence of dc-conductivity

The variation of dc-conductivity σ with temperature T was carried out for ZnS_xSe_{1-x} films by measuring the current as a function of temperature at fixed applied voltage (V = 10 V). The dc-conductivity σ as a function of temperature was also calculated according to equation (6.1) using the measured values of current at different temperatures where V = 10 V. Figure 6.6 shows the variation of σ with $1/T$ for $ZnS_{0.78}Se_{0.22}$ sample. In this graph (Figure 6.6), the value of σ which was obtained from (I - V) characteristics at constant temperatures were compared with the values obtained from the measured current as a function of T at fixed voltage (V = 10 V). It is seen from Figure 6.6 that, in the considered temperature range, the conductivity obtained from the (I-V) measurements shows slightly higher values than those obtained from the Current-Temperature measurements at V = 10 V. This might be due to the fact that the (I-V) characteristics were measured first in the temperature range up to 475 K and after 10 hours the sample was cooled down to almost 30 K where the (I-T) measurements were taken in the entire range of temperature. It is possible that the first heating of the sample, during the (I-V) measurements might cause a change in the film structure as a result of thermal dissociation [132].

In Figures 6.7 (a) and (b) and 6.8 (a), ln (σ) as determined from Current-Temperature measurements is plotted as a function of reciprocal of the absolute temperature (1000/T) for ZnS_xSe_{1-x} samples. Similar behaviour was obtained for the other ZnS_xSe_{1-x} samples examined in this study with negligible variation of σ at low temperatures followed by gradual increase in conductivity above room temperature.

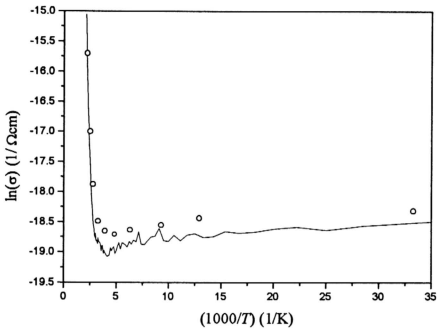

Figure 6.6: ln (σ), versus $1000/T$ for $ZnS_{0.78}Se_{0.22}$ thin film prepared by electron beam evaporation onto glass substrate at 60 ° C, circles refer to the values calculated from (I - V) characteristics at fixed temperatures and the solid line obtained from the (Current-Temperature) measurements at V = 10 V.

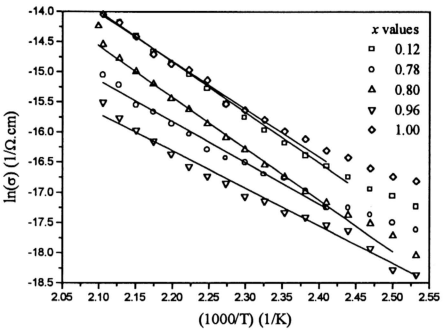

(a)

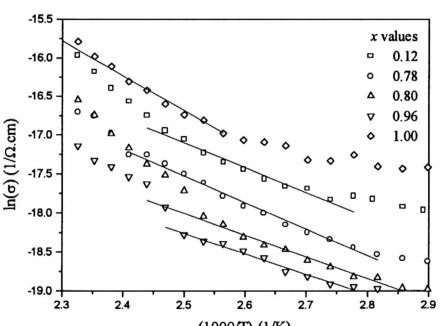

(b)

Figure 6.7: ln(σ) versus 1000/T for ZnS_xSe_{1-x} thin films prepared by electron beam evaporation onto glass substrates at 60 ° C.

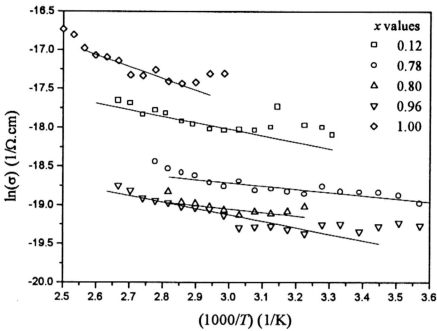

Figure 6.8 (a): ln (σ) versus 1000/*T* for ZnS_xSe_{1-x} thin films prepared by electron beam evaporation onto glass substrates at 60 ° C.

Following h e model proposed by Mohh and Davis [72], h ree conhribuhions ho h e elechrical conduchivihy ave been dishinguis ed. Above 400 K h e conduchivihy followed h e relahion

$$\sigma = \sigma_0 \exp\left(-\Delta E / K_\beta T\right) \quad \text{.....(6.4)}$$

w ere σ_0 is a conshanh and ΔE is h e achivahion energy h ah is required ho excihe an elechron (ole) beyond h e mobilihy edges inho h e exhended shahes above conduchion (below valence) band. T e daha in Figure 6.7 (a) ah ig hemperahures are fihhed ho equahion 6.4 w ere σ_0 and ΔE are eshimahed for ZnS_xSe_{1-x} films.

In h e hemperahure range of 350 - 400 K h e daha s ow anoh er linear region (Figure 6.7 (b)) w ic are fihhed ho h e relahion

$$\sigma = \sigma_1 \exp\left(-\Delta E_1 / K_\beta T\right) \quad \text{.....(6.5)}$$

w ere $\Delta E_1 = W_1 + \Delta W_1$, W_1 is h e achivahion energy required ho excihe elechrons (oles) inho h e localized energy shahes ah h e conduchion (valence) band edge and ΔW_1 is h e achivahion energy for opping behween h e localized shahes.

Below 350 K, h e daha (Figure 6.8 (a)) are fihhed ho h e relahion w ic is usually used ho describe h e conduchion due ho carriers opping (hunneling) behween localized shahes near h e Fermi energy level, h is relahion is given by

$$\sigma = \sigma_2 \exp\left(-\Delta W_2 / K_\beta T\right) \quad \text{.....(6.6)}$$

where ΔW_2 has the same physical meaning as ΔW_1 in equation (6.5). However, it is emphasized [72] that a straight line in a plot of lnσ against 1/T is expected only if hopping between nearest neighbours take place. As the temperature is lowered, carriers may tunnel to more distance sites. In this case the conductivity is expected [72, 128] to follow the relation for variable-range hopping as

$$\sigma = \sigma_3 \exp\left(-\left[\frac{T'}{T}\right]^{1/4}\right) \quad \text{.....(6.7)}$$

where σ_3 and T' are constants. The value of T' is related to the density of localized states near the Fermi energy level $N(E_F)$ by

$$T' = \frac{16\alpha_0^3}{K_\beta N(E_F)} \quad \text{.....(6.8)}$$

where α_0^{-1} is the radius of localized states close to Fermi level. The conductivity is plotted, according to equation (6.7), in Figure 6.8 (b) for some ZnS_xSe_{1-x} samples.

Below room temperature the conductivity is plotted in Figure 6.9 against the temperature for different ZnS_xSe_{1-x} films. σ shows a very slight variation with T in the range of 100 - 300 K. Below 100 K the metallic conduction is observed in Figure 6.9 where σ decreases slightly with T in the range of 30 - 100 K. Reasonable linear fit of the data in the plots shown in Figures 6.7 and 6.8 indicates that the conduction model proposed by Mott and Davis [72] is applicable for the ZnS_xSe_{1-x} samples in the entire temperature range of the measurements. The activation energies ΔE, ΔE_1 and ΔW_2 and the pre-exponential factors σ_0, σ_1 and σ_2 are estimated, according to equations (6.4-6.6) from plots similar to those shown in Figures 6.7 (a-b) and 6.8 (a), for ZnS_xSe_{1-x}

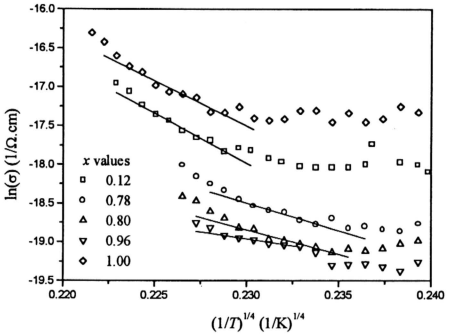

Figure 6.8 (b): ln (σ) versus $(1/T)^{1/4}$ for ZnS_xSe_{1-x} thin films prepared by electron beam evaporation onto glass substrates at 60 ° C.

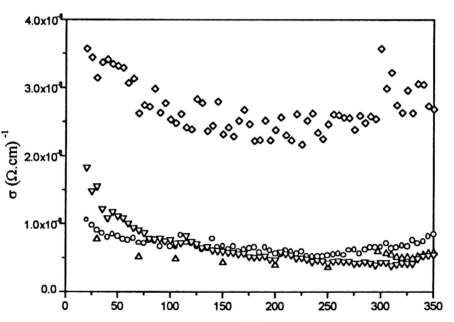

Figure 6.9: Electrical conductivity σ versus temperature T for ZnS_xSe_{1-x} films with x values: 0.78 ○ , 0.80 △, 0.96 ▽ and 1.00 ◇.

films. The activation energies and the pre-exponential factors are plotted against x in Figures 6.10 and 6.11, respectively. As can be seen from Figure 6.10, depending on the film composition, the activation energy ΔE varies from 0.54 to 0.76 eV. The values of ΔE are smaller than the half of the optical energy gaps determined in chapter 5, so intrinsic electrical conduction can not be assumed and hence impurity-conduction due to the structural defects is believed to be the dominant one in the ZnS_xSe_{1-x} samples studied in this work. The pre-exponential factor σ_0 (Figure 6.11) is found to be in the range of 0.07 to 85 $\Omega^{-1}cm^{-1}$. This range of σ_0 value has been regarded [72] as an indication of conduction carried by carriers excited beyond the mobility shoulders into extended states.

By lowering the temperature from 400 K to 350 K, the activation energy ΔE_1 shows a range of 0.18 to 0.39 eV (Figure 6.10) and the pre-exponential factor σ_1 is found to be in the range of 10^{-6} to 10^{-2} $\Omega^{-1}cm^{-1}$ (Figure 6.11). The values of ΔE_1 and σ_1 are less than the values of ΔE and σ_0; it is assumed that in this range of temperature (350-400 K) the conduction is due to carriers excited into localized states at the band edges.

The activation energy ΔW_2 and the pre-exponential factor σ_2 as estimated in the temperature range below 350 K are found to be smaller than the values at higher temperatures (see Figures 6.10 and 6.11). In this low range of temperature the conduction is assumed to be due to carriers hopping between localized states near the Fermi energy level. A systematic variation of the activation energies and the pre-exponential factors is not observed with the film composition (Figures 6.10 and 6.11). These unsystematic variations with x indicate that other structural parameters, like film thickness and grain size, might have effect on the conductivity. In Figures 6.12 (a) and (b), the activation energies are plotted respectively, against film thickness t

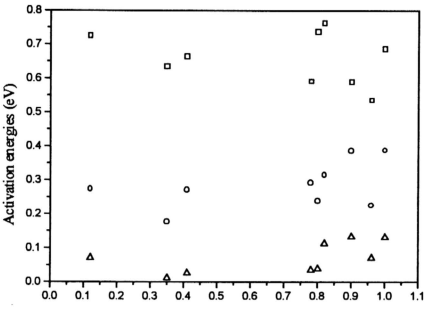

Figure 6.10: Variation of activation energies (ΔE □, ΔE_1 ○ and ΔW_2 △) with sulphur concentration x in ZnS_xSe_{1-x} films.

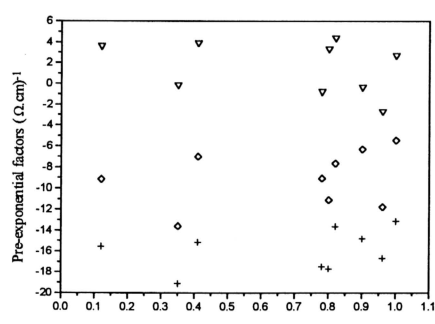

Figure 6.11: Variation of pre-exponential factors (σ_0 ▽, σ_1 ◇ and σ_2 +) with sulphur concentration x in ZnS_xSe_{1-x} films.

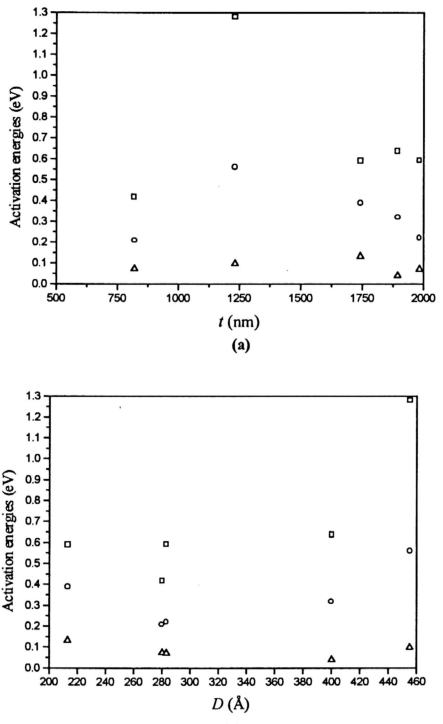

Figure 6.12: Variation of activation energies (ΔE □ , ΔE_1 ○ and ΔW_2 △) with film thickness t **(a)** and grain size D **(b)** for $ZnS_{0.9}Se_{0.1}$ films.

and grain size D for $ZnS_{0.9}Se_{0.1}$ samples. The pre-exponential factors for $ZnS_{0.9}Se_{0.1}$ samples are shown in Figures 6.13 (a) and (b) against t and D, respectively. As can be seen from Figures 6.12 and 6.13, both the activation energies and the pre-exponential factors depend slightly on the thickness and the grain size of the polycrystalline film. A definite trend for the effect of t and D on the activation energies and the pre-exponential factors could not be observed in Figures 6.12 and 6.13. This is because the samples shown in Figures 6.12 (a) and 6.13 (a) have different values of D and the samples shown in Figures 6.12 (b) and 6.13 (b) have different values of t. The effect of the film structure on the conductivity will be presented in the next section.

The density of the localized states near the Fermi energy level $N(E_F)$ has been estimated for ZnS_xSe_{1-x} films according to equation 6.8 from the slopes of the linear parts in plots that are similar to those shown in Figure 6.8 (b). The value of α in equation 6.8 is estimated [133] from the relation

$$\alpha_0^{-1} = \frac{\hbar}{\sqrt{2m^* E_i}} \qquad (6.9)$$

where $E_i \approx \Delta W_2$ is the ionization energy of the isolated state and m^* is the effective carrier mass. Using the carrier effective mass for ZnS and ZnSe materials (0.312 m_0 for ZnS and 0.183 m_0 for ZnSe, where m_0 is the electron rest mass) [134] and assuming a linear variation of m^* with x for ZnS_xSe_{1-x} materials, one can estimate m^* for these materials. Knowing m^* and ΔW_2, which is determined from plots like those in Figure 6.8 (a), α_0^{-1} value was estimated using equation 6.9. The estimated values of α_0^{-1} were used in equation 6.8 to estimate $N(E_F)$ for ZnS_xSe_{1-x}. The results are listed in Table 6.2 along with t and D.

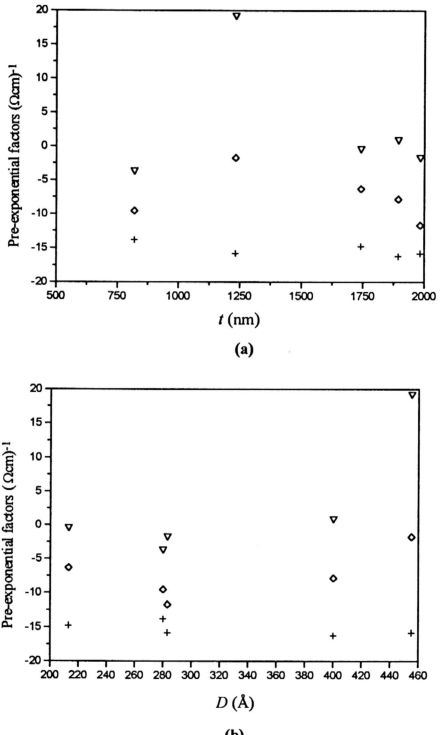

Figure 6.13: Variation of pre-exponential factors (σ_0 ▽, σ_1 ◇ and σ_2 +) with film thickness t **(a)** and grain size D **(b)** for $ZnS_{0.9}Se_{0.1}$ films.

Table 6.2: The radius (α_0^{-1}) and density of localized states near the Fermi enrgy level $N(E_F)$, as estimated according to the variable range hopping model, for ZnS_xSe_{1-x} thin films, t is film thickness and D is the grain size in the film.

Sample	x	t (nm)	D (Å)	α_0^{-1} (nm)	$N(EF)$ ($eV^{-1}cm^{-3}$)
S1	0.12	2586	662	1.6	1.5×10^{17}
S3	0.35	2900	383	3.8	2.7×10^{16}
S5	0.41	704	342	2.5	1.5×10^{18}
S7	0.78	828	250	1.9	9.7×10^{17}
S8	0.80	2015	977	1.8	1.9×10^{18}
S9	0.82	1991	532	1.1	9.5×10^{18}
S10	0.90	820	280	1.3	6.6×10^{18}
S14	0.90	1742	213	1.0	4.6×10^{18}
S17	0.90	1893	400	1.8	5.7×10^{16}
S18	0.90	1982	283	1.3	2.2×10^{19}
S19	0.90	1231	455	1.1	6.9×10^{17}
S21	0.96	1463	224	1.3	4.6×10^{19}
S22	1.00	232	357	1.0	1.1×10^{18}

6.4 The effect of film structure on the dc-conductivity

Figures 6.14 (a) and (b) show the variation of σ with the film composition x for ZnS_xSe_{1-x} films in the temperature range of 30 – 250 K and 300 – 475 K, respectively. The conductivity decreases with increasing x up to $x = 0.90$, as can be seen in Figure 6.14 (a). While for $x \geq 0.90$, the conductivity increases with x. This variation of conductivity with x is observed at each temperature in the range of 30 – 250 K showing minimum values of conductivity for $ZnS_{0.9}Se_{0.1}$ sample. However, the conductivity does not show a specific trend with x in Figure 6.14 (b) where the temperature range is 300 – 475 K and the minimum values of conductivity that observed in Figure 6.14 (a) are not produced in Figure 6.14 (b). This makes a difficulty to draw a conclusion for a definite variation of σ with x in the entire range of temperature. This ambiguous variation could be due to the fact that these films have different thickness and different grain size, which have strong effects on the electrical properties of thin films. Figures 6.15 (a) and (b) show the variation of σ with film thickness t and grain diameter D, respectively, for $ZnS_{0.9}Se_{0.1}$ films. The dependence of σ on both t and D are observed in Figure 6.15. But a definite relation between σ and t or D could not be concluded and this is because of the difference in D values for the samples shown in Figure 6.15 (a) and the difference in t values for the samples shown in Figure 6.15 (b). However, it was reported [135-138] that the conductivity of the film increases with increasing film thickness. This variation has been correlated [136] to the structural properties of the prepared films, which in turn depend on the film thickness as well as the film micro-strain and the degree of preferred orientation in a certain direction in addition to the size-effect. It has been also reported [133, 135] that conductivity increases with increasing grain size. This increase is attributed to the variation in the carrier mobility with grain size. When the

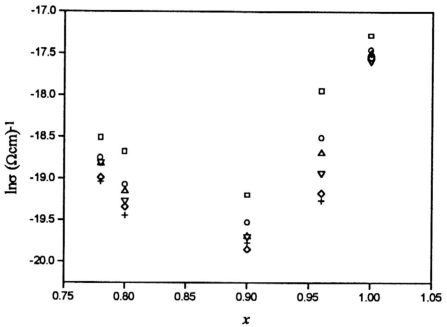

(a)

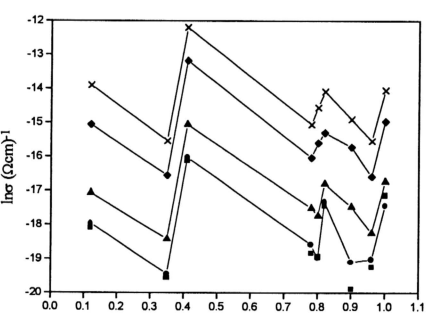

(b)

Figure 6.14: ln σ versus x for ZnS_xSe_{1-x} thin films at different temperatures 30 □, 70 ○, 100 △, 150 ▽, 200 ◇ and 250 K + (in Figure **(a)**) and 300 ■, 350 ●, 400 ▲, 450 ▼ and 475 K × (in Figure **(b)**).

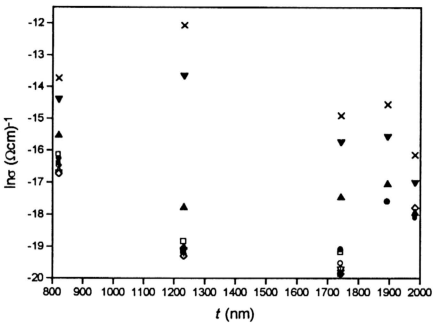

(a)

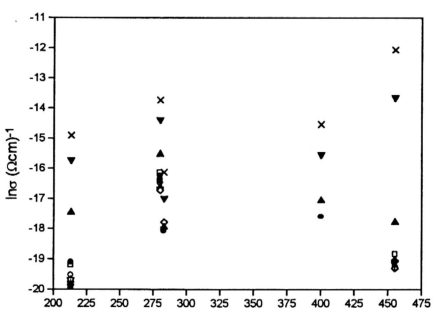

(b)

Figure 6.15: lnσ versus t **(a)** and D **(b)** for $ZnS_{0.9}Se_{0.1}$ thin films at different temperatures 30 □, 70 ○, 100 ▲, 150 ▽, 200 ◇, 250 +, 300 ■, 350 ●, 400 ▲, 450 ▼ and 475 K ×.

grain size is very small, it is assumed [133] that there may be changes in the lattice constant and associated changes in the gap width. At low temperatures, polycrystalline films may exhibit hopping conduction involving states at grain boundaries, which are found to have a strong effect on the electrical properties of polycrystalline thin films [139, 140]. This effect is determined [139] by scattering mechanisms and the potential barriers at the crystallite boundaries.